IN-SITU REAL TIME MONITORING OF THE POLYMERIZATION IN GEL-CAST CERAMIC PROCESSES

S. Ahuja, S. L. Dieckman, G. A. Bostrom, L. G. Waterfield, A. C. Raptis, and
O. O. Omatete[†]
Energy Technology Division
Argonne National Laboratory
Argonne IL 60439-4825

[†]Metals and Ceramics Division, Oak Ridge National Laboratory, Oak Ridge TN.

ABSTRACT

The method of gelcasting requires making a mixture of a slurry of ceramic powder in a solution of organic monomers and casting it in a mold. Gelcasting is different from injection molding in that it separates mold filling from setting during conversion of the ceramic slurry to a formed green part. In this work, nuclear magnetic resonance (NMR) spectroscopy and imaging has been used for in-situ monitoring of the gelation process and gelcasting of alumina. ^{1}H NMR spectra and images are obtained during polymerization of a mixture of soluble reactive acrylamide monomers. Polymerization was initiated by adding an initiator and an accelerator to form long-chain, cross-linked polymers. Multidimensional NMR imaging was utilized for in-situ monitoring of the process and for verification of homogeneous polymerization. Comparison of the modeled intensities with acquired images shows a direct extraction of T_1 data from the images.

INTRODUCTION

Copolymerization of methacrylamide (MAA) and N,N'-methylene bisacrylamide (MBAA) has been of interest in making strong, machinable polymeric parts [1]. Both aqueous (water-based) versions, as in traditional ceramic processing, and nonaqueous (organic-solvent-based) versions of MAA-MBAA copolymerization have been studied. Gelcasting is a ceramic forming process in which a slurry of ceramic powder is mixed in a solution of organic monomers and

DISCLAIMER

DISCLAIMER

Portions of this document may be illegible in electronic image products. Images are produced from the best available original document.

the mixture is cast into a mold [1, 2]. As indicated in the flow-chart of the process, shown in Fig. 1, the ceramic powder, organic monomers (binders), a solvent, and a dispersant are mixed to form a slurry. The initiator is added to the slurry to begin the polymerization and the mixture is transferred into a mold for casting. After the mixture is cast, the slurry is converted into a gel, which holds the ceramic particles in shape. The mold is removed and the specimen is dried in a controlled atmosphere to remove the solvent. The organic monomers (binders) are then burned off and the specimen is sintered to form a dense part.

Organic solvents are used in nonaqueous gelcasting. If water is employed as the solvent, the process is termed aqueous gelcasting. As mentioned earlier, aqueous gelcasting has a number of advantages over nonaqueous gelcasting processes. In the aqueous gelcasting process, monofunctional monomers MAA and difunctional MBAA are premixed using the solvent water, AP is added to the premix to initiate the polymerization and the catalyst TEMED is used to accelerate the polymerization process. The gelation process is usually exothermic and the gels formed are transparent and form homogeneously in the solution without a gelation front and without phase separation. To make ceramic parts, alumina powder is added to the premix and Darvan C is added as a dispersant prior to adding the initiator and the accelerator. The mixture is then poured into a preheated plastic, metal, wax, or glass mold. In this case, the slurry gels into a green part with no noticeable defects or porosities, even when complex molds are employed.

The difference between traditional ceramic processing and the acrylamide gelcasting technique is that the MAA and MBAA monomers replace the poly(vinyl alcohol) used as a binder.

The relaxation effects in the polymeric network are directly correlated with the polymerization process. This paper is concerned with aqueous polymerization because the use of water as a solvent facilitates drying and disposal while reducing overall viscosity. In this work, multidimensional nuclear magnetic resonance (NMR) imaging was conducted to characterize polymerization homogeneity and because in-situ study of the polymerization process was necessary. The varying relaxation effects, especially the spin-lattice relaxation time in the premix have been determined by NMR spectroscopy.

High-resolution ^{1}H NMR spectroscopy has been used to study the cross-linking polymerization of acrylamide (AA) and MBAA to measure the composition of a residual comonomer mixture during and after polymerization [3]. Cross-linking polymers and polymeric gels have been used extensively because of their chemical and physical properties. The physical properties of polymeric gels have been determined by applying NMR to study the motional state of water and the polymer network [4]. Low-temperature studies of aqueous solutions of AA and MBAA with AP and TEMED have shown that polymerization of cross-linked polyacrylamide (PA) to form cryogels is complex involving chemical and physical

```
┌──────────────┐   ┌──────────────┐   ┌─────────────────────────────────┐
│Ceramic Powder│   │   Organic    │   │Solvent (nonaqueous and aqueous) │
│              │   │  Monomers    │   │           Dispersant            │
│              │   │  (binders)   │   │                                 │
└──────────────┘   └──────────────┘   └─────────────────────────────────┘
```
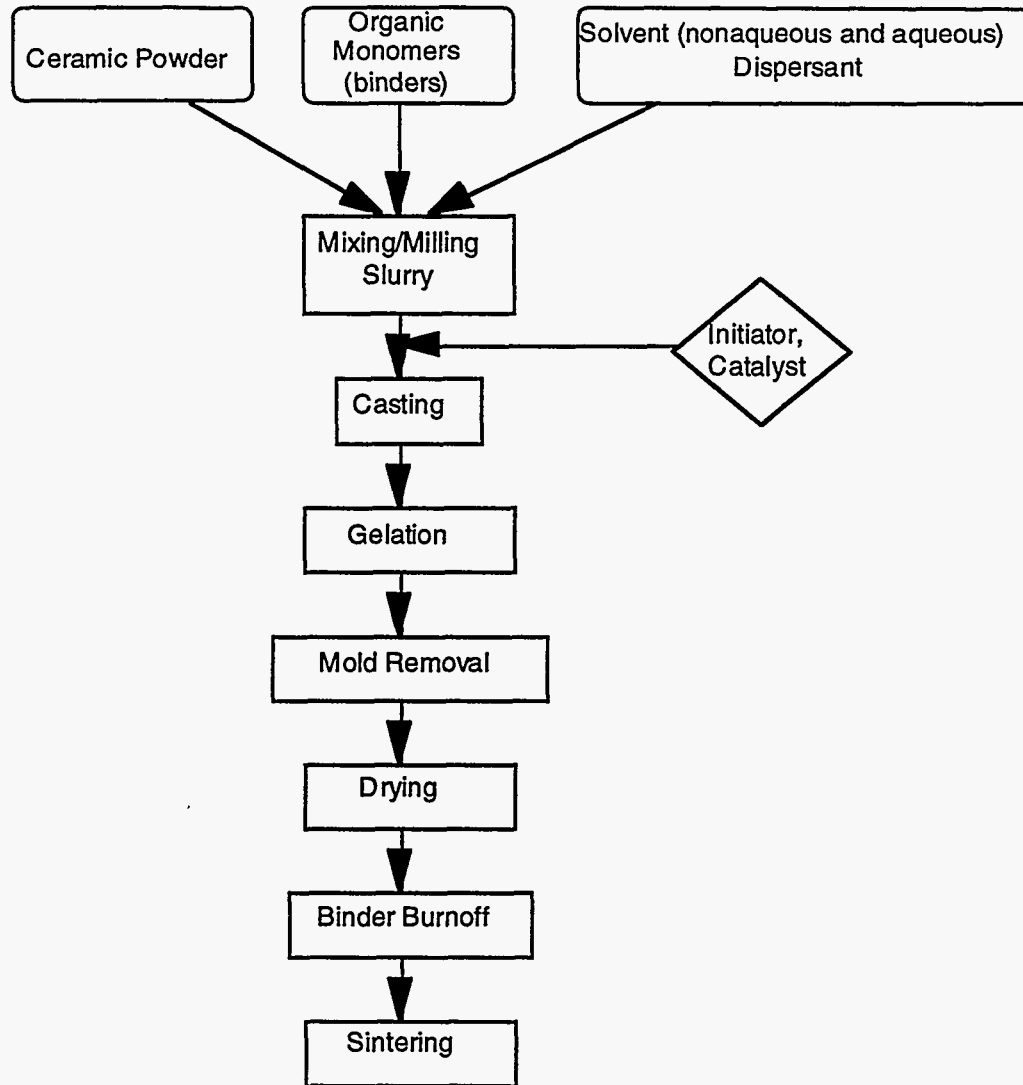
Fig. 1. Flowchart for gelcasting process. (adapted from Ref. 1)

phenomena. Furthermore, the dynamics of polymerization depend on the thermal history of the sample [5]. In this work, multidimensional nuclear magnetic resonance (NMR) imaging was conducted to characterize polymerization homogeneity and because in-situ study of the polymerization process was necessary.

EXPERIMENTAL ASPECTS

High-resolution NMR spectrometry of an MAA-MBAA copolymer mix was performed on a Bruker AP-300 spectrometer with a commercial probe at a magnetic field strength of 7.1 T. Low-resolution NMR spectroscopy and imaging studies were conducted on a Tecmag NMR Kit II and Libra data acquisition system interacting with a CXP-100 spectrometer and a Macintosh Quadra 950 computer. Spectra and images at a magnetic field strength of 35 T were obtained by an in-house-built imaging accessory [6] tuned to the proton resonance frequency of 100.13 MHz. Orthogonal linear magnetic field gradients across the specimen were driven by three 1000-W Techron audio amplifiers. A sequence of spectra was acquired with varying interpulse delay times, τ. Delay times of 2, 5, 20, 50, 200, and 500 ms, and 2, 5, 10 and 20 s were used in the sequence to obtain 2-D images. For each time delay, the time domain data matrix of 128 x 128 was obtained by accumulating eight transients. The total time for data acquisition was 139 min. Room-temperature shims were used to acquire good free-induction decay (FID) on a water sample and the data matrix was made symmetrical by adjusting the field gradients, thus evolving a central image of a slice of a sample cross section.

The samples were prepared from soluble reactive AA (monomer) and MBAA (cross-linking molecules), and the premix was made with water as the solvent [1]. The initiator, 10% AP, and the accelerator TEMED were then added to begin polymerizing the monomers, which formed long-chain, cross-linked polymers. For high resolution, 5 mm-diameter NMR sample tubes were used; for low resolution, the solution was transferred to a 15-mm diameter, cylindrical, flat-bottomed tube and placed rapidly in the probe for spectroscopy experiments. For low-resolution imaging experiments, it was necessary to obtain a corresponding contrast between the polymerized and nonpolymerized specimens. For this reason, the sample geometry was such that MAA-MBAA without the initiator was placed in a small-diameter inner tube (5 mm) immersed in a larger diameter (15-mm) tube that contained polymerizing MAA-MBAA and the initiator. The time of the initial measurement was recorded and careful monitoring of the polymerization was conducted with respect to time. Times were subsequently recorded at the end of an experiment and at the beginning of the next computer-controlled experiment.

^{1}H NMR studies of T_1 were conducted on the individual standard MAA-MBAA copolymer premix at a magnetic field strength of 7.1 T. Spectra were acquired with D_2O as the solvent at 35°C to suppress the observable solvent resonance. The standard inversion recovery NMR pulse technique was employed for these studies. NMR spectroscopy and imaging procedures were performed at 25 and 35°C to determine the variation in T_1 and whether the polymerization is homogeneous. The measurements of T_1 reveal the effect of polymerization on the

motion of the methyl group and the side and main chains [7]. T_1 measurements can be used to determine changes in molecular motion caused by polymerization [8].

RESULTS AND DISCUSSION

NMR spectra were studied as a function of the extent of MAA-MBAA polymerization. The ^{1}H NMR spectra were acquired on individual standard MAA-MBAA reagents and on composite copolymer premix reagents. Spectra were acquired with H_2O (as solvent) at ambient temperature and at 35°C. The standard inversion recovery NMR pulse technique, employed for the measurement of spin-lattice relaxation time, T_1, utilized a 180° pulse, followed by a time delay, τ, then another 90° pulse (180°-τ-90°-acquire). T_1 is a measure of the time taken for transfer of energy to or from the lattice; i.e., for the spin system to approach thermal equilibrium. In these studies, real-time ^{1}H NMR spectra of the copolymerization reaction were acquired as a function of reaction time. The spectra demonstrate a reduction in methylene and methyl resonances as the polymerization reaction progresses. A variation of the spin-lattice relaxation rates of the components as a function of reaction extent is also expected.

NMR imaging was conducted on MAA-MBAA prepared in water. During imaging, the obtained NMR signal was due largely to water in the premix and overwhelmed the signal due to other constituents in the premix. A T_1 inversion recovery sequence 90°-τ-composite 180° indicates delays and gradient activation at specific intervals. Figure 2 shows a sequence of 2-D ^{1}H NMR images of the MAA-MBAA polymerization reaction with time in the frequency domain. These were obtained by Fourier transformation of 2-D spectra initially acquired in the time domain. All of the images show the concentration gradient in the specimen.

Figure 2(a) shows a 2-D ^{1}H NMR image of the MAA-MBAA copolymer premix at O min. Here, the polymerization has not begun because the initiator and the accelerator have not begun to react with the copolymer premix. During the process, at any temperature, no polymerizing front was observed with imaging techniques, and polymer gels formed homogeneously throughout the solution. It may be noted that the distortion at the periphery of the sample is an artifact of the imaging experiment and relates to the limitation of tuning of the gradient coils in the probe assembly. The sequence of images shows that because of the polymerization, relaxation occurred more rapidly in the polymerizing MAA-MBAA (i.e., in the outer tube) than in the inner tube where the relaxation remained constant.

Because the images are individually scaled in intensity, it appears that the image intensity of the inner tube decreases. The images also demonstrate the actual time of polymerization. At time O min, the concentration of the polymerizing specimen in the outer tube was essentially the same as the concentration of the raw
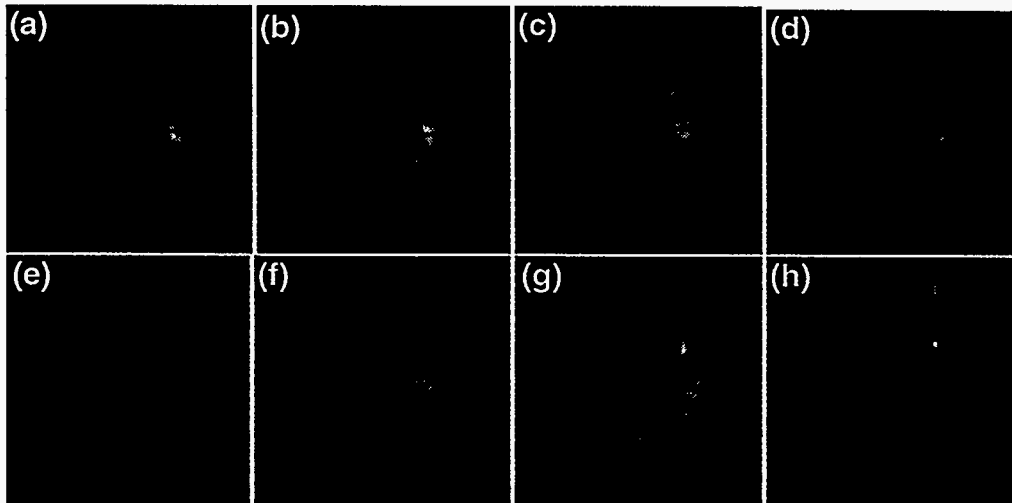
Fig. 2. 2-D ^{1}H NMR images at times (a) 0 min, (b) 26 min, (c) 45 min, (d) 64 min, (e) 83 min, (f) 102 min, (g) 120 min, and (h) 138 min of standard MAA-MBAA polymerization reaction with initiator.
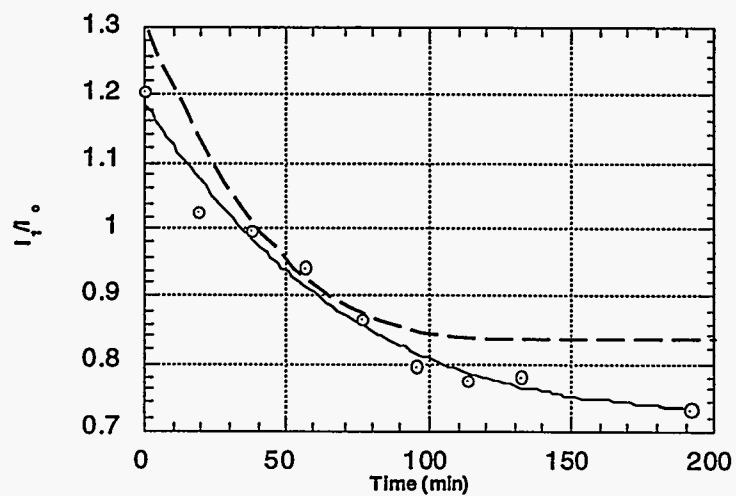

Fig. 3. Ratio of intensities of polymerizing MAA-MBAA (I_1) to uninitiated MAA-MBAA (I_o) vs. time: solid line = experimental plot derived from images in Fig. 1; dashed line = theoretical plot of image intensity.

specimen without initiator in the inner tube, as seen in Fig. 2(a). As polymerization continues, the specimen in the outer tube becomes more viscous, which leads to the intermediate intensity shown in Fig. 2(e) at 83 min. Complete polymerization takes place at 138 min, as shown in Fig. 2(h). The intensities of the images vary with further acquisition of images. Variation of intensity is shown in Fig. 3 by a plot of the intensity ratio (outside intensity/inside intensity, I_1/I_0) vs. time as the polymerization occurred. Intensity variation corresponds to that from a simple spherical domain with an exterior sink. If the material is inhomogeneous, the magnetization or intensity decay can be expected to be a composite sum of two exponentials [9]. The curvature in the intensity-vs-time plot for the MAA-MBAA system strongly indicates that the system is inhomogeneous. The signal intensity [10], taking $T_2 \gg \tau$, is

$$S \propto \left(2e^{\tau/2T_1} - 1\right)\left(\rho e^{-T_I/T_1} + e^{-\tau_{tot}/T_1}\right). \tag{1}$$

The relationship in Eq. 1 shows the codependency of T_1 with the intensity of the obtained images. Figure 3 (dashed line) shows a plot of the intensity vs. time according to Eq. 1 for corresponding values of T_1. The decrease in intensity corresponds to the images shown in Fig. 2 and the intensity variation (solid line) shown in Fig. 3. In future work, we will analyze nonaqueous gel systems that include alumina solid loading and composites, as well as the concentration differences between the raw specimen and the polymerizing specimen, to understand how the main quantity of comonomers becomes involved in the polymerization process. T_2 values will be determined and the fitting analysis recomputed to understand the differences between the solid and the dashed lines in Fig. 3.

Acknowledgments

REFERENCES

1. O. O. Omatete, M. A. Janney, and R. A. Strehlow, *Am. Ceram. Soc. Bull.,* **70** (10) 1641-1649 (1991).

2. A. C. Young, O. O. Omatete, M. A. Janney, and P. A. Menchhofer, *J. Am. Ceram. Soc.*, **74** (3) 612-18 (1991).
3. J. L. Nieto, J. Baselga, I. H-Fuentes, M. A. Llorente, and I. F. Pierola, *Eur. Polym. J.*, **23** (7) 551-555 (1987).
4. H. Tanaka, K. Fukumori, and T. Nishi, *J. Chem. Phys.*, **89** 3363-3372 (1988).
5. D. G. Gusev, V. I. Lozinsky, and V. I. Bakhmutov, *Eur. Polym. J.*, **29** 49-55 (1993).
6. N. Gopalsami, G. A. Foster, S. L. Dieckman, W. A. Ellingson, and R. E. Botto, *Review of Progress in Quantitative Nondestructive Evaluation*, D. O. Thompson and D. E. Climenti, eds., Plenum Press, New York, **9A** 861-868 (1990).
7. A. Charlesby, *Radiat. Phys. Chem.*, **26** 463 (1985).
8. J. W. Harrell, Jr., and S. Ahuja, *Chem. Phys.*, **138** (1989) 383-390.
9. D. C. Douglass, *Polymer Characterization by ESR and NMR*, A. E. Woodward and F. A. Bovey, eds., ACS Symposium Series 142, American Chemical Society, Washington, DC, 147-168 (1980).
10. F. O. Garces, K. Sivadasan, P. Somasundaran and N. J. Turro, *Macromolecules*, **27** 272-278 (1994).